Proceedings of the Eighteenth International Conference on
Civil, Structural and Environmental Engineering Computing
Edited by: P. Iványi, J. Kruis and B.H.V. Topping
Civil-Comp Conferences, Volume 10, Paper 9.2
Civil-Comp Press, Edinburgh, United Kingdom, 2025
ISSN: 2753-3239, doi: 10.4203/ccc.10.9.2

Random Forest-Based Surrogate Modeling of Blast Parameters from Cuboid Charges

T. H. Lee, Y. Lee and J.-W. Hong

Department of Civil and Environmental Engineering, KAIST, Daejeon, Republic of Korea

Abstract

Assessing the blast resistance of reinforced concrete slabs is crucial for protecting infrastructure against increasing risks from explosions and industrial hazards. The complex behavior of slabs under blast loading, particularly when subjected to cuboid-shaped charges, poses significant challenges for conventional experimental and numerical methods. We develop a surrogate model that conducts high-fidelity arbitrary Lagrangian-Eulerian (ALE) simulation results with machine learning techniques to predict key blast parameters such as the arrival time, peak time, peak pressure, decay duration, and impulse across a wide range of charge geometries. A total of 363 simulations are conducted by systematically varying the length, width, and height of cuboid-shaped charges to generate the dataset. Using the random forest algorithm, the surrogate model generates pressure-time history curves, which are verified against numerical simulation results. This study provides an efficient approach for evaluating blast loading on critical structures and contributes to the enhancement of safety design.

Keywords: blast simulation, arbitrary Lagrangian-Eulerian method, machine learning, random forest, reinforced concrete, surrogate modeling.

1 Introduction

Among various structural elements, reinforced concrete (RC) slabs are widely used and are exposed to the risk of external blast loads. Research on measuring blast responses and predicting the behavior of RC slabs has become essential for evaluating explosion-induced damage. Numerous experimental studies have investigated the interactions between RC slabs and blast phenomena [1, 2, 3]. However, full-scale blast tests are costly, pose significant safety concerns, and produce highly uncertain measurements due to the extreme speed and intensity of chemical explosion reactions. In recent decades, researchers have developed empirical models to address these limitations. One of the most widely used tools is conventional weapons (CONWEP), produced by the U.S. Department of Defense. This military code implements the Kingery–Bulmash equation, which establishes mathematical relationships between charge weight, standoff distance, and blast pressure [4]. However, CONWEP assumes that explosive charges are spherical. In practical applications, charges are usually cylindrical or cuboid. Consequently, assuming a spherical charge may lead to inaccurate results. Therefore, in recent years, researchers have shifted from empirical models to physics-based numerical analyses that incorporate both solid and fluid mechanics [5, 6, 7, 8, 9]. Although these advanced simulations can represent fluid-structure interactions more realistically, they require extensive computational resources, limiting their practical applicability. Machine learning-based surrogate modeling provides an effective alternative by reducing computational demands.

In this research, a machine learning model is trained by high-fidelity numerical simulation data, enabling efficient prediction of blast parameters [10, 11, 12, 13]. We develop a surrogate model to predict the blast parameters imposed on RC slabs by cuboid-shaped charges under varying geometric conditions. A high-fidelity numerical model based on the arbitrary Lagrangian-Eulerian (ALE) method is established to simulate blast loading on RC slabs in an open field, and is verified against experimental data by comparing peak pressure, as referenced in [14]. To generate the dataset required for machine learning, the length, width, and height of the cuboid-shaped charge are systematically varied across multiple simulations. From each simulation, a pressure-time history curve is obtained, and key blast parameters, including arrival time, peak time, peak pressure, decay duration, and impulse, are extracted. A random forest algorithm is employed, and parameters from the resulting model are utilized to develop a pressure-time history generation process for cuboid-shaped charges. This methodology enhances both accuracy and computational efficiency, providing a robust foundation for further advancements in numerical simulations for blast resistance design.

2 Methodology

2.1 Conservation equations with ALE formulation

In open fields, an explosion can be modeled as a fluid flow comprising both the explosive charge and the surrounding air. The governing equations in the fluid domain, including the conservation equations for mass, momentum, and energy, are expressed as [15]

$$\frac{\partial \rho}{\partial t} = -\rho \nabla \cdot \mathbf{v} - \mathbf{w} \cdot \nabla \rho, \tag{1}$$

$$\rho \frac{\partial \mathbf{v}}{\partial t} = \nabla \cdot \boldsymbol{\sigma} + \rho \mathbf{b} - \rho \big(\mathbf{w} \cdot \nabla\big)\mathbf{v}, \tag{2}$$

$$\rho \frac{\partial E}{\partial t} = \boldsymbol{\sigma} : \nabla \mathbf{v} + \rho \mathbf{b} \cdot \mathbf{v} - \rho \big(\mathbf{w} \cdot \nabla\big) E, \tag{3}$$

where ρ is the material density, t is time, $\mathbf{v}$ is the material velocity vector, $\mathbf{u}$ is the element velocity vector, $\mathbf{w} = \mathbf{v} - \mathbf{u}$ is the relative velocity vector, $\boldsymbol{\sigma}$ denotes the stress tensor, $\mathbf{b}$ represents the volumetric force vector acting on the fluid elements, and E is the energy. The stress tensor $\boldsymbol{\sigma}$ is given by

$$\boldsymbol{\sigma} = -p\mathbf{I} + \mu \Big(\nabla \mathbf{v} + (\nabla \mathbf{v})^T\Big), \tag{4}$$

where p is the fluid pressure and μ is the dynamic viscosity.

To effectively manage large deformations in blast simulations, the Arbitrary Lagrangian-Eulerian (ALE) formulation combines the Lagrangian and Eulerian methods [16]. The ALE approach uses the Lagrangian method during small deformations, preserving mesh-material correspondence, thus simplifying the conservation equations as

$$\frac{\partial \rho}{\partial t} = -\rho \nabla \cdot \mathbf{v}, \tag{5}$$

$$\rho \frac{\partial \mathbf{v}}{\partial t} = \nabla \cdot \boldsymbol{\sigma} + \rho \mathbf{b}, \tag{6}$$

$$\rho \frac{\partial E}{\partial t} = \boldsymbol{\sigma} : \nabla \mathbf{v} + \rho \mathbf{b} \cdot \mathbf{v}. \tag{7}$$

When severe element distortion occurs, the distorted mesh is updated, and a remapping step solves the pure advection equations for ρ, $\rho\mathbf{v}$, and ρE, transferring material information onto the rezoned mesh. Because $\mathbf{w} \neq 0$, the advection terms are reappeared as

$$\frac{\partial \rho}{\partial t} + \nabla \cdot \big(\rho \mathbf{w}\big) = 0, \tag{8}$$

$$\frac{\partial (\rho \mathbf{v})}{\partial t} + \nabla \cdot \big(\rho \mathbf{v} \mathbf{w}\big) = 0, \tag{9}$$

$$\frac{\partial (\rho E)}{\partial t} + \nabla \cdot \big(\rho E \mathbf{w}\big) = 0. \tag{10}$$

2.2 Machine learning models

In this study, a random forest algorithm is utilized to predict blast parameters using the geometric variables of the cuboid-shaped charge. The random forest algorithm is based on a decision tree algorithm, and the decision tree selects a feature and splitting criterion to partition the input data into smaller subsets, reducing variance in regression problems. As the splitting process continues, the tree grows deeper. When a predefined stopping criterion is met, the process stops, forming leaf nodes. The input data are partitioned into J disjoint regions $\{R_1, R_2, \ldots, R_J\}$, each corresponding to a leaf node. The function $h(\mathbf{x})$ of the tree can be written as

$$\begin{aligned} h(\mathbf{x}) &= \hat{y}_1 \quad \text{if } \mathbf{x} \in R_1, \\ h(\mathbf{x}) &= \hat{y}_2 \quad \text{if } \mathbf{x} \in R_2, \\ &\vdots \\ h(\mathbf{x}) &= \hat{y}_J \quad \text{if } \mathbf{x} \in R_J, \end{aligned} \tag{11}$$

where R_j is the region associated with the j-th leaf node and $\hat{y}_j$ is value assigned to that node. The random forest regression aggregates multiple decision trees by a bagging process [17]. Bagging splits data into smaller subsets, randomly inputs them into decision trees, and synthesizes the output values. If the result from the m-th decision tree is denoted as $h_m(\mathbf{x})$, the final result $f(\mathbf{x})$ is computed as

$$f\left(\mathbf{x}\right) = \frac{1}{M} \sum_{m=1}^{M} h_m\left(\mathbf{x}\right), \tag{12}$$

where M is the number of decision trees. Machine learning algorithm is trained to minimize the mean squared error (MSE) loss function, defined as

$$\mathrm{MSE} = \frac{1}{N} \sum_{i=1}^{N} \left(y_i - f\left(\mathbf{x}_i\right)\right)^2, \tag{13}$$

where N is the number of test samples. The MSE places a heavier penalty on larger errors than on smaller ones due to the squared residuals, making the model more sensitive to outliers.

3 Numerical simulation

3.1 Numerical model

The numerical model is developed based on field blast tests reported in Ref. [14]. The slabs measured 1,100 $\times$ 1,000 $\times$ 40 mm^3 and contained a single layer of reinforcing bar mesh positioned near the bottom face. The steel bars had a diameter of 6 mm, an elastic modulus of 210 GPa, and a yield strength of 653.4 MPa. The bars were spaced

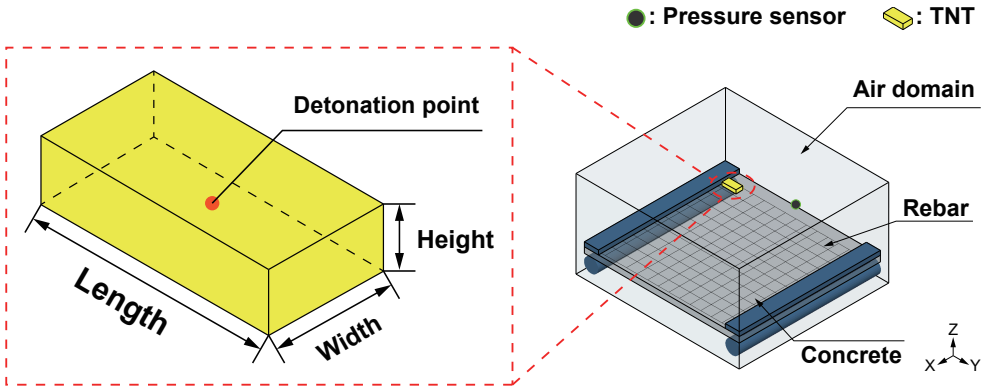

Figure 1: Configuration of numerical model.

at 75 mm intervals. The slabs were simply supported by a steel frame with a span of 1,000 mm. TNT was used as the explosive charge, with a detonation velocity of 6,730 m/s and a density of 1.6 g/cm^3. The standoff distance between the charge and the slab surface was maintained at 400 mm, while the charge weights were varied at 200 g, 400 g, and 600 g. During the experiments, the maximum blast pressure was recorded by a sensor mounted on the slab.

The configuration of the numerical model, which consists of both structural and fluid components, is shown in Fig. 1. In the structural component, the slab and support are modeled by 8-node hexahedral elements, while the reinforcing mesh is represented by 2-node beam elements. Instead of sharing nodes, constraints in solid elements are applied between steel beams and concrete solids to synchronize their movements, accurately simulating an RC structure. The slab and support are modeled with an element size of 5 mm, whereas the beam element had an element size of 2.5 mm to capture the detailed behavior of the reinforcement. In the fluid component, the air domain is modeled to include both the RC slab and the explosive charge, with an element size of 5 mm.

The continuous surface cap model (CSCM) is used to accurately simulate the nonlinear behavior of concrete structures under blast loading conditions [18, 19, 20]. The rebar and steel frame are modeled by a bilinear elastic-plastic model, commonly employed to simulate isotropic and kinematic hardening plasticity [21]. To simulate the fluid material, an equation of state (EOS) is defined [22]. Air is modeled by a linear polynomial EOS, whereas the explosive charge behavior is represented by the Jones-Wilkins-Lee (JWL) EOS. The air domain is modeled by the null material model, which enables the application of the linear polynomial EOS without calculating deviatoric stresses. To simulate TNT detonation, a high-charge burn model is employed based on the research of Wilkins.

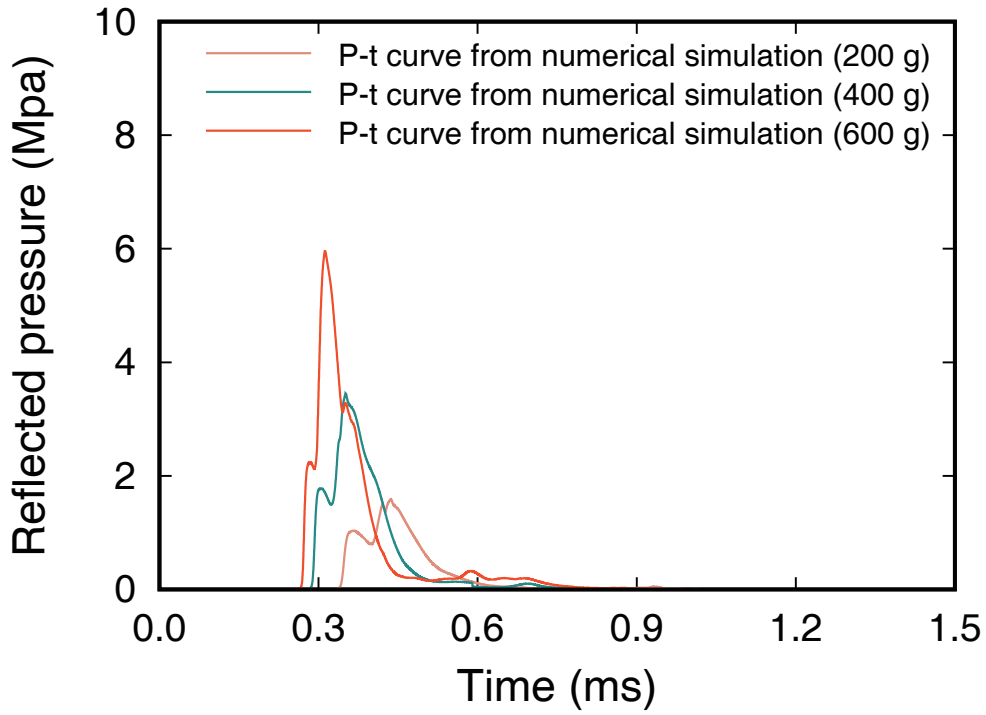

Figure 2: Time history curves for reflected pressure considering charge weight.

3.2 Model verification

The time histories of the reflected pressures and impulses for various charge weights are shown in Fig. 2. An increase in the charge weight leads to a higher peak pressure and earlier arrival of the shockwave at the sensor. Heavier charges release more blast energy, which strengthens the shock front and accelerates its propagation, thereby reducing the time required to reach the sensor. The pressure then undergoes a decay phase, which decreases over time.

Experimental measurements of the peak pressure along with the results from ALE-based high-fidelity numerical models are listed in Table 1. The ALE-based numerical model considers a cuboid geometry, resulting in an error of less than 5% for all charge weights. Because the actual shape of the explosives are considered, the ALE-based numerical simulations provide accurate blast pressure results.

Table 1: Comparison of experimental peak pressures with results from the ALE-based numerical model [14].

Charge weight (g)	Experiment (MPa)	Numerical simulation (MPa)	Error (%)
200	1.62	1.59	1.69
400	3.60	3.45	4.13
600	5.88	5.96	1.30

4 Machine learning and surrogate model

4.1 Machine learning model and training results

Three input parameters length L, width W, and height H are systematically sampled within realistic manufacturing limits to form the dataset for the machine learning models. One dimension is fixed at the base size $\sqrt[3]{\frac{M_e}{\rho_e}}$, where M_e denotes the charge weight and ρ_e the density of charge. The other two vary according to a dimension ratio that takes 21 distinct values from 1.0 to 3.0 in increments of 0.25 and from 3.0 to 9.0 in increments of 0.5. Each of these dimension ratios is paired with its reciprocal, yielding a total of 121 unique shapes. When combined with three different charge weights, 200 g, 400 g, and 600 g, the result is 363 scenarios in total.

The five blast parameters are set as the output parameters obtained from the pressure-time history curve. The parameter t_a is the arrival time of the shockwave, which marks the moment when the pressure begins to increase. The peak time t_p represents the moment at which the pressure reaches its maximum value during the positive phase. The decay duration t_d means the interval from the peak pressure to the moment when the pressure returns to ambient level. The variable P_s stands for the peak pressure, indicating the peak pressure achieved during the blast. Finally, the impulse I, defined as the area under the pressure-time history curve, quantifies the total energy transmitted.

Preprocessing consists of three steps. First, the outliers are removed from the output data. Next, the input variables are standardized. Finally, the output values are transformed to achieve the desired scale. As the outputs are positive, a logarithmic transformation is applied to convert them before training the model. After the model makes results in this transformed space, the values are converted back to their original scale by applying an exponential transformation. Cross-validation is an additional step for enhancing the performance of machine learning algorithms. For cross-validation, the training dataset is partitioned into k^{cv} equally sized folds [23]. The function is trained on $k^{\text{cv}} - 1$ folds, and the remaining fold is used for validation. Each fold is tested once and the resulting MSE values are averaged to evaluate the overall performance of the algorithms. In this study, k^{cv} is set as 10.

The scatter plots in Fig. 3 show the performance of the output parameters, and the results obtained by the random forest algorithm, shown in Fig. 16, are significantly closer to the reference line, showing superior performance.

4.2 Pressure time history generation process

A random forest algorithm is employed to build a surrogate model that predicts key blast parameters for various charge configurations. These parameters are used to construct the positive phase pressure time history in two parts. A cubic equation is used for the steep pressure rise, and the Friedlander equation is used for the subsequent decay. From the arrival time t_a to the peak pressure time t_p, the pressure rise is

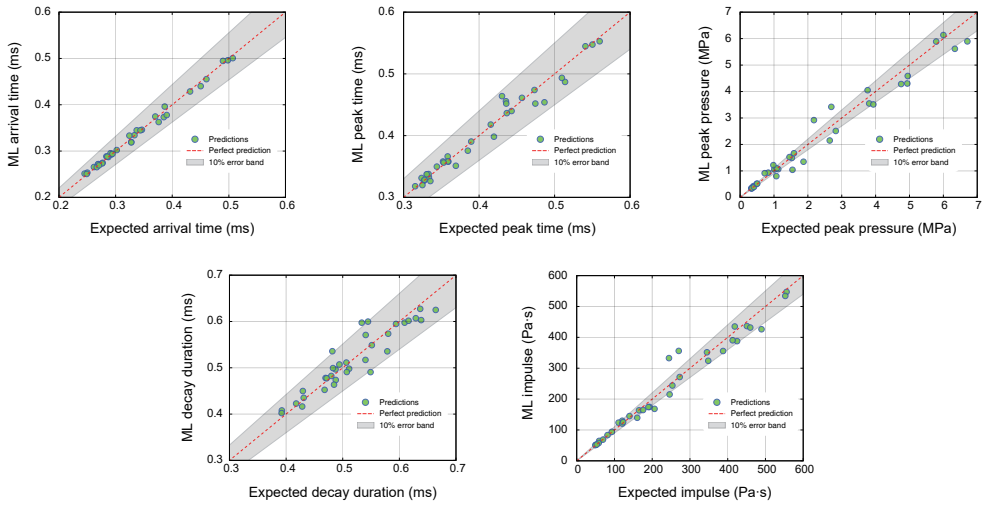

Figure 3: Predicted vs. calculated scatter plot of output parameters in random forest regression.

expressed as

$$p(t) = a\,(t - t_a)^3, \quad t_a < t \leq t_p, \tag{14}$$

where a is the cubic coefficient determined by the results of the surrogate model t_a, t_p, and the peak pressure P_s. The partial impulse during this rise interval is given by

$$I_{\text{rise}} = \int_{t_a}^{t_p} a\,(t - t_a)^3\,dt. \tag{15}$$

After the pressure reaches its peak at t_p, the Friedlander equation, which is widely employed in blast analyses [24, 25], is used to describe the decay from t_p to $t_p + t_d$ and is given by

$$p(t) = P_s\Big(1 - \frac{t - t_p}{t_d}\Big)\,\exp\Big[-\alpha\,\Big(\frac{t - t_p}{t_d}\Big)\Big], \quad t_p < t \leq t_p + t_d, \tag{16}$$

where t_d is the decay duration and α is the decay constant. The impulse in this decay interval is then computed as

$$I_{\text{decay}} = \int_{t_p}^{t_p + t_d} P_s\Big(1 - \frac{t - t_p}{t_d}\Big)\,\exp\Big[-\alpha\,\Big(\frac{t - t_p}{t_d}\Big)\Big]\,\mathrm{d}t. \tag{17}$$

The overall positive phase blast load from the arrival time t_a to the end of the decay is shown in Fig. 4.

A random sample from the test dataset is selected to evaluate whether the surrogate model can predict the pressure–time history curve. The sample is a 200 g TNT charge, and its length is seven times greater than its height. A comparison between

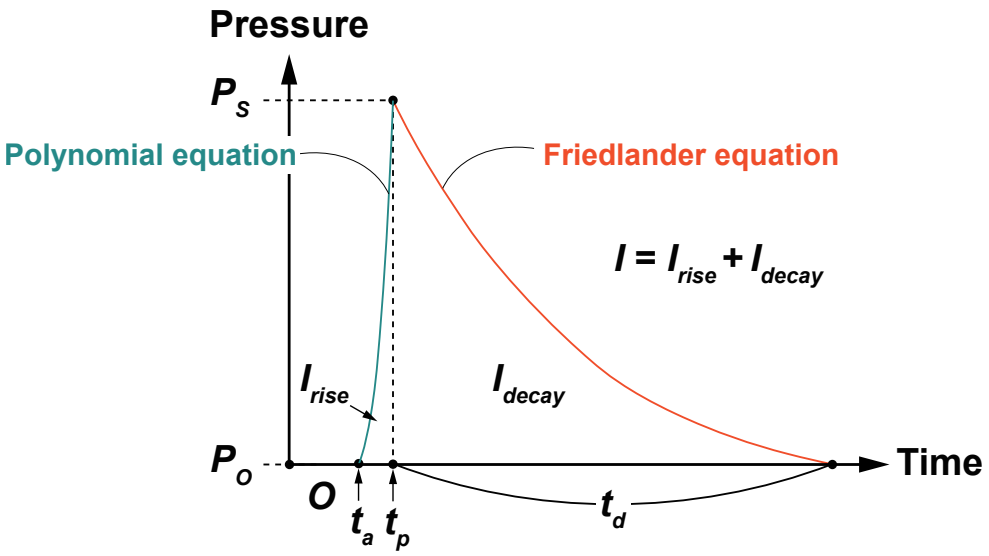

Figure 4: Schematic of the rise and decay of the positive phase blast pressure.

the pressure-time history curves generated by the surrogate model and those obtained from the high-fidelity numerical simulations for the three different samples is shown in Fig. 5. The surrogate model produces pressure-time history curves that closely match those derived from the ALE-based numerical simulation.

5 Concluding remarks

We develop a surrogate model that efficiently simulates blast loading on RC slabs while considering the geometry of cuboid-shaped charges. High-fidelity ALE simulations are conducted with machine learning techniques to create an effective model. An ALE-based numerical model is developed to simulate blast loading on an RC slab using cuboid charges of 200 g, 400 g, and 600 g. The model is verified by comparing peak pressure against experimental data. By systematically varying the charge length, width, and height, 363 cases are simulated. Key blast parameters, including arrival time, peak time, peak pressure, decay duration, and impulse, are extracted to construct a comprehensive dataset for machine learning. Subsequently, a random forest algorithm is rigorously trained on these data. This carefully optimized model achieves highly accurate results, as evidenced by the strong alignment between predicted and simulated blast parameters. The pressure-time history curve is generated by substituting the random forest-predicted blast parameters into the equation, which unifies the cubic-Friedlander hybrid equation, producing results closely aligned with those from ALE simulations.

High-fidelity ALE simulations demonstrate that physics-based numerical methods can accurately reproduce complex blast phenomena. Specifically, simulations utilizing the ALE method effectively capture the intricate behavior of blast wave

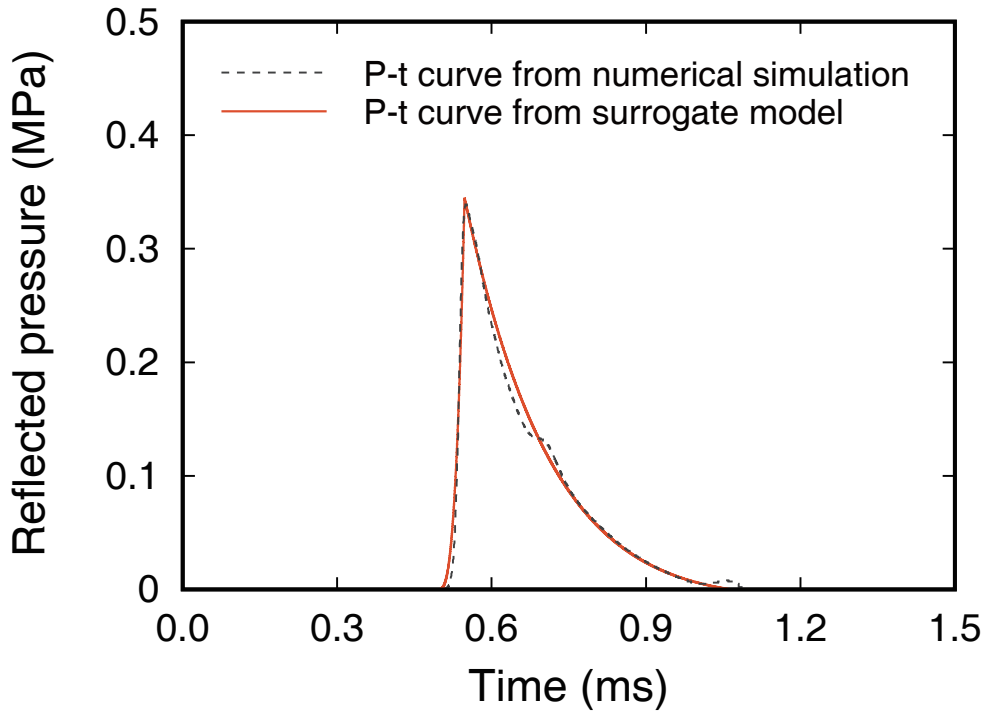

Figure 5: Comparison of pressure-time history curves generated by the surrogate model and numerical simulations.

propagation and its interaction with reinforced concrete slabs. By incorporating detailed fluid-structure interactions, ALE simulations provide highly accurate results of peak pressure, achieving excellent agreement with experimental data. These results confirm that physics-based simulations are essential for reliably predicting blast effects, particularly when precise evaluation of structural responses is required. Consequently, physics-based simulations not only provide trustworthy data for detailed blast analysis but also serve as a foundation for developing efficient surrogate models.

The hybrid surrogate modeling approach, integrating machine learning results with the cubic-Friedlander hybrid equation, is verified as an effective methodology for predicting blast pressure-time histories. By employing key parameters through the random forest algorithm, including arrival time, peak time, peak pressure, decay duration, and impulse, in conjunction with the cubic-Friedlander hybrid equation, the surrogate model produces pressure-time curves closely matching those obtained from high-fidelity ALE simulations. This combined approach significantly reduces computational costs while maintaining the accuracy, highlighting its practical applicability. Ultimately, this surrogate modeling framework can facilitate real-time blast response analyses and support optimized safety design practices under various explosive loading conditions.

Acknowledgements

This work was supported by the Nuclear Safety Research Program through the Korea Foundation Of Nuclear Safety (KoFONS) using the financial resource granted by the Nuclear Safety and Security Commission (NSSC) of the Republic of Korea (No. 00242257) and also supported by the National Research Foundation of Korea (NRF) grant funded by the Korea government (MSIT) (No. 2022R1A2C2091533).

References

[1] Z. Guo, Z. Xu, C. Chen, B. Zhang, D. E. Lehman, & S. Cao, "Behavior of GFRP retrofitted reinforced concrete slabs subjected to conventional explosive blast," *Materials and Structures*, 50, 1-15, 2017.

[2] A. Maazoun, B. Belkassem, B. Reymen, S. Matthys, J. Vantomme, & D. Lecompte, "Blast response of RC slabs with externally bonded reinforcement: Experimental and analytical verification," *Composite Structures*, 200, 246-257, 2018.

[3] J. Ning, S. Yang, T. Ma, & X. Xu, "Fragment behavior of concrete slab subjected to blast loading," *Engineering Failure Analysis*, 138, 106370, 2022.

[4] C. Kingery, G. Bulmash, "Technical report ARBRL-TR-02555: Air blast parameters from TNT spherical air burst and hemispherical burst," *AD-B082*, 713.

[5] A. Dua, A. Braimah, M. Kumar, "Experimental and numerical investigation of rectangular reinforced concrete columns under contact explosion effects," *Engineering Structures*, 205, 109891, 2020.

[6] S. Rigby, C. Osborne, G. Langdon, S. Cooke, D. Pope, "Spherical equivalence of cylindrical explosives: Effect of charge shape on deflection of blast-loaded plates," *International Journal of Impact Engineering*, 155, 103892, 2021.

[7] L. Gan, Z. Zong, J. Lin, Y. Chen, M. Xia, L. Chen, "Influence of U-shaped stiffeners on the blast-resistance performance of steel plates," *Journal of Constructional Steel Research*, 188, 107046, 2022.

[8] Y. Fan, L. Chen, Z. Li, H.-b. Xiang, Q. Fang, "Modeling the blast load induced by a close-in explosion considering cylindrical charge parameters," *Defence Technology*, 24, 83–108, 2023.

[9] L. Gan, Z. Zong, Z. Chen, T. Wu, J. Lin, M. Li, "Differences in responses of square steel plates exposed to blast loads generated by cubic and spherical explosives," *Thin-Walled Structures*, 182, 110332, 2023.

[10] C. Zhao, Y. Zhu, Z. Zhou, "Machine learning-based approaches for predicting the dynamic response of RC slabs under blast loads," *Engineering Structures*, 273, 115104, 2022.

[11] J. Furtney, C. Thielsen, W. Fu, R. Le Goc, "Surrogate models in rock and soil mechanics: Integrating numerical modeling and machine learning," *Rock Mechanics and Rock Engineering*, 1–15, 2022.

[12] N. A. Nariman, M. Husek, A. M. Ramadan, ”Surrogate models for the damage responses of a reinforced concrete beam under explosive charges utilizing coupled finite element–stochastic methods,” *Engineering with Computers*, 39 (1), 285–305, 2023.

[13] H. Kim, D.-H. Han, T. H. Lee, J.-W. Hong, ”An application of machine learning for geometric optimization of a dual-throat bent nozzle,” *Advances in Engineering Software*, 202, 103869, 2025.

[14] J. Feng, Y. Zhou, P. Wang, B. Wang, J. Zhou, H. Chen, H. Fan, F. Jin, ”Experimental research on blast-resistance of one-way concrete slabs reinforced by BFRP bars under close-in explosion,” *Engineering Structures*, 150, 550–561, 2017.

[15] H. Louahlia-Gualous, M. Asbik, ”Numerical modeling of annular film condensation inside a miniature tube,” *Numerical Heat Transfer, Part A: Applications*, 52 (3), 251–273, 2007.

[16] M. Souli, A. Ouahsine, L. Lewin, ”ALE formulation for fluid–structure interaction problems,” *Computer Methods in Applied Mechanics and Engineering*, 190 (5-7), 659–675, 2000.

[17] G. Biau, E. Scornet, ”A random forest guided tour,” *Test*, 25, 197–227, 2016.

[18] J.-W. Jung, Y.-C. Yoon, H. W. Jang, J.-W. Hong, ”Investigation on the resistance of steel-plate concrete walls under high-velocity impact,” *Journal of Constructional Steel Research*, 162, 105732, 2019.

[19] D. Park, T. H. Lee, Y. Lee, Y. Choi, J.-W. Hong, ”Blast simulations of a reinforced concrete slab using the continuous surface cap model (CSCM),” *Journal of Building Engineering*, 96, 110603, 2024.

[20] D. Park, S. Kim, S. Jin, Y. Choi, H. Kim, J.-W. Hong, ”Seismic vulnerability assessment of leaning U-shaped masonry fence walls,” *Earthquake Spectra*, 87552930251320413, 2025.

[21] K. Ko, S. Jin, S. E. Lee, J.-W. Hong, ”Impact resistance of nacre-like composites diversely patterned by 3D printing,” *Composite Structures*, 238, 111951, 2020.

[22] R. Panciroli, S. Abrate, G. Minak, A. Zucchelli, ”Hydroelasticity in water-entry problems: Comparison between experimental and SPH results”, *Composite Structures*, 94 (2), 532–539, 2012.

[23] D. R. Roberts, V. Bahn, S. Ciuti, M. S. Boyce, J. Elith, G. Guillera-Arroita, S. Hauenstein, J. J. Lahoz-Monfort, B. Schr¨oder, W. Thuiller, *et al.*, ”Cross-validation strategies for data with temporal, spatial, hierarchical, or phylogenetic structure,” *Ecography*, 40 (8), 913–929, 2017.

[24] F. G. Friedlander, ”The diffraction of sound pulses I. Diffraction by a semi-infinite plane,” *Proceedings of the Royal Society of London. Series A. Mathematical and Physical Sciences*, 186 (1006), 322–344, 1946.

[25] A. Ullah, F. Ahmad, H.-W. Jang, S.-W. Kim, J.-W. Hong, ”Review of analytical and empirical estimations for incident blast pressure,” *KSCE Journal of Civil Engineering*, 21 (6), 2211–2225, 2017.